

# Analyst

Accepted Manuscript



This is an *Accepted Manuscript*, which has been through the Royal Society of Chemistry peer review process and has been accepted for publication.

*Accepted Manuscripts* are published online shortly after acceptance, before technical editing, formatting and proof reading. Using this free service, authors can make their results available to the community, in citable form, before we publish the edited article. We will replace this *Accepted Manuscript* with the edited and formatted *Advance Article* as soon as it is available.

You can find more information about *Accepted Manuscripts* in the [Information for Authors](#).

Please note that technical editing may introduce minor changes to the text and/or graphics, which may alter content. The journal's standard [Terms & Conditions](#) and the [Ethical guidelines](#) still apply. In no event shall the Royal Society of Chemistry be held responsible for any errors or omissions in this *Accepted Manuscript* or any consequences arising from the use of any information it contains.

Cite this: DOI: 10.1039/c0xx00000x

www.rsc.org/xxxxxx

ARTICLE TYPE

## The disordered silver nanowires membrane for extraction surface-enhanced Raman spectroscopy detection

Yu-e Shi,<sup>a</sup> Limei Li,<sup>b</sup> Min Yang,<sup>a</sup> Xiaohong Jiang,<sup>a</sup> Quanqin Zhao,<sup>a</sup> Jinhua Zhan<sup>\*a</sup>*Received (in XXX, XXX) Xth XXXXXXXXX 20XX, Accepted Xth XXXXXXXXX 20XX*

DOI: 10.1039/b000000x

The disordered silver nanowires membrane combining the solid-phase extraction (SPE) with surface-enhanced Raman spectroscopy (SERS) was used for rapid collection and detection of food contaminants. The membrane was fabricated via filtering the silver nanowires colloid solution, which was prepared by solve-thermal polyol process. Analytes in 5 mL liquid phase were concentrated in less than 10 s by the affinity of silver nanowires on filter membrane. The membrane could combine the advantages of SPE and SERS technology for analysis of the food safety contaminants. The employment of the SERS-active extraction membrane eliminated the procedure of elution, which shortened the time of the analysis. It has been shown that the as-prepared membrane had good uniformity and high temporal stability under continuous laser radiation. Qualitative and quantitative detection of phorate and melamine was further performed based on flow-through method. The characteristic SERS intensity against phorate and melamine concentrations exhibited a good linear relationship in the concentration range of 2.5 to 10  $\mu\text{g}\cdot\text{mL}^{-1}$  (phorate) and 2.5 to 100  $\mu\text{g}\cdot\text{mL}^{-1}$  (melamine).

### Introduction

As the global food industry continues to expand, food safety analysis has attracted worldwide attention. It is important to develop sensitive, rapid and efficient methods for detecting the concentration of food contaminants.<sup>1</sup> At the laboratory level, food safety, which implies biological, detrimental, and chemical factors, can be quantitatively assessed by many methods, including cell culture and instrumental analysis.<sup>2</sup> These methods require several hours or days to analysis. What is more, some contaminants are in ultralow level, in order to improve the sensitivity of contaminants assays, a sample pre-concentration step is usually employed. Among these methods, solid-phase extraction (SPE) is commonly used to pre-concentrate organic chemicals extremely.<sup>3</sup> Coupled with high performance liquid chromatography (HPLC) or mass spectrometry (MS), SPE has been used for enriching some contaminants.<sup>4-7</sup> The most commonly used sorbents are porous silica media modified with organic group such as alkyl groups which could be used to extract the target compounds with nonpolar or weakly polar from the polarity matrix. Carbon nanotubes, as a typical one dimensional nanomaterial, had also been used as adsorbents for trapping or separation of highly polar compounds in the last few years.<sup>8,9</sup> Surface enhanced Raman spectroscopy (SERS) had emerged as an alternative sensing technique for its unique features, such as high sensitivity, unique spectroscopic fingerprint.<sup>10,11</sup> It had attracted much attention and found its application in various fields,

such as environmental analyses, biomedical applications and cultural heritage studies.<sup>12-15</sup> Moreover, SERS could also be used as an on-site and nondestructive data acquisition technique.<sup>16-22</sup> The highly effective SERS-active system is attributed to the surface plasmon resonance (SPR) of the closely connected nanostructures with the field enhancement within them.<sup>23,24</sup> It is considered that the SPRs are tunable from the visible to near-IR regions of the spectrum by controlling the shape or size of the metallic nanoparticles,<sup>25</sup> and selecting the shape-controllable metallic nanoparticles as the SERS substrates can contribute to maximizing the Raman signal of the analytes. The most widely used SERS substrates are metallic nanoparticles with a large size distribution and various shapes prepared by wet chemical methods. Silver nanostructures embedded filter paper as SERS substrate through adsorption or filtration of performed silver colloid has been reported.<sup>26-32</sup>

Silver nanowires have the certain aspect ratio, which are easily loaded on the membrane substrate.<sup>33-37</sup> Herein, we reported the facile fabrication of the disordered silver nanowires extraction membrane, which could combine the advantages of SPE and SERS technology for analysis of contaminants. The employment of the disordered silver nanowires extraction membrane eliminated the procedure of elution, which shortened the analysis time. The temporal stability under continuous laser radiation, uniformity and reproducibility of the SERS-active extraction membrane were demonstrated. This membrane provides a rapid and sensitive platform for the SERS detection of the contaminants in the water sample.

## Experimental

### Chemicals

Silver nitrate ( $\text{AgNO}_3$ , 99.8%), ethylene glycol (EG, 99.0%), potassium chloride (KCl) polyvinylpyrrolidone K-30 (PVP,  $M_w=55000$ ) and ethanol were all purchased from Sinopharm Chemical Reagent CO. Ltd. (Shanghai, China). P-Aminothiophenol (PATP, 97%) and phorate were purchased from Sigma-aldrich. Organic membranes (Nylon, 25 mm diameter,  $0.22 \mu\text{m}$  pore size) were purchased from New Asia purification device factory (Shanghai, China). Ultra-pure water ( $18.25 \text{ M}\Omega\cdot\text{cm}$ ) was used throughout the experiment.

### Preparation of silver nanowires

Silver nanowires were prepared by a solve-thermal polyol process according to the reported method.<sup>38</sup> In a typical synthesis, a transparent solution of PVP (0.4 M, 80 mL) and KCl (0.002 M, 80 mL) was prepared using ethylene glycol as the solvent at  $80 \square$ . A solution of silver nitrate (0.067 M, 120 mL) was prepared at room temperature. The former solution was added drop-wise into  $\text{AgNO}_3$  solution under vigorous stirring. The mixed solution was placed overnight and transferred into a 250 mL autoclave. The autoclave was placed into the oven and kept at  $160 \square$  for 7 h. The solution was then cooled to room temperature. The nanowires were centrifuged (2000 rpm, 30 min) and washed three times with ethanol. The centrifuged silver nanowires were dispersed into 50 mL ethanol.

### Fabrication of the silver nanowires membrane and detection of sample

The silver nanowires membrane was used as the SERS-active substrate in this work, which had high SERS activity. The preparation of the substrate was based on the flow through method. In brief, the organic filter membrane was put into a suitable filter paper holder. 1.5 mL silver nanowires colloid was inhaled to injector, and then the filter paper holder was attached to the injector. After that, silver nanowires colloid was passed through the filter membrane. The silver nanowires were trapped on the filter membrane, which could be used as an SERS-active extraction membrane.

The SERS performance of the silver nanowires membrane was evaluated using PATP as the probe. The extraction effect of the membrane by filtering or immersing the sample solution was also compared. As for the filtering method, after the analytes in aqueous solution have passed through the membrane, the filter paper holder was removed. The membrane was dried in air and analyzed using the SERS detection equipment. Qualitative and quantitative detection of phorate and melamine in aqueous solution using this membrane were also performed using the filter method.

### Substrate characterization and SERS detection

The prepared silver nanowires were characterized by X-ray diffraction (XRD) using a Bruker D8 advanced X-ray diffractometer equipped with graphite monochromatized  $\text{Cu K}\alpha$  radiation ( $\lambda=1.5418 \text{ \AA}$ ). The morphology of the silver nanowires membrane was characterized using a Scanning electron microscope (JSM-6700F). All SERS measurements were attached to an Ocean Optics QE65000 spectrometer with the excitation wavelength of 785 nm. The excitation power was 180 mW and the integration time was 1 s.

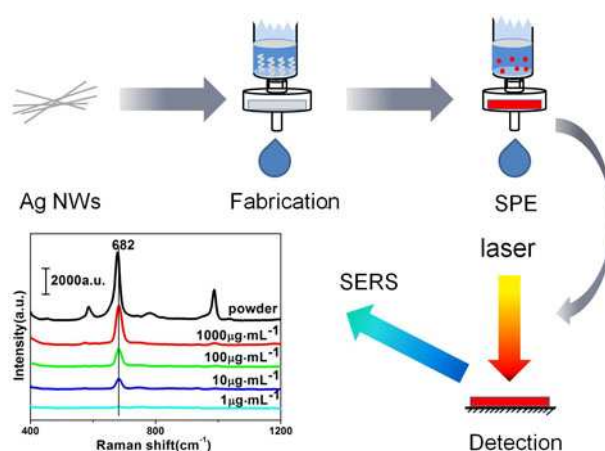


Fig. 1 Illustration of silver nanowires loaded on organic filter membrane used as flow-through SERS.

## Results and discussion

### Fabrication and characterizations of the SERS-active extraction membrane

Fig. 1 gave a schematic of the preparation of the silver nanowires membrane and detection of samples. The silver nanowires membrane was prepared by filtering the silver nanowires colloid. Fig.S1 shows the intensity of the  $1076 \text{ cm}^{-1}$  PATP Raman peak after first loading increasing volumes of silver nanowires colloid through the filter membrane. The Raman signal intensity increased significantly less than 1.5 mL of silver nanowires colloid, the Raman signal intensity is unchanged when more than 2.0 mL. Therefore, for all subsequent experiments, 1.5 mL of silver nanowires colloid was selected through the filter membrane. Silver nanowires loaded on organic filter membrane with inherent porosity were used as the SERS-active substrate, thus combining rapid collection of the analytes with in situ detection. The membrane could combine the advantages of SPE and SERS technology for analysis of food contaminants. The employment of the silver nanowires extract membrane eliminated the procedure of elution, which shortened the analysis time.

The structure of the silver nanowires was characterized by XRD as shown in Fig. 2A. All peaks could be readily indexed to cubic-phase Ag, according to standard JCPDS card no. 04-0783, indicating that the silver nanowires were finely crystallized and successfully synthesized by the solve-thermal method. UV-vis absorption spectrum of the silver nanowires aqueous solution had the two characteristic peaks at 378 nm and 351 nm in Fig.S2.<sup>39</sup> The morphology of the silver nanowires membrane was characterized by SEM. Fig. 2B showed that this membrane was consist of the interwoven uniform silver nanowires with  $\sim 50 \text{ nm}$  in diameter and  $\sim 5 \mu\text{m}$  in length. Inset showed the photo of the silver nanowires membrane. The thickness of the silver nanowires membrane was about  $10 \mu\text{m}$  in Fig.S4.

### Uniformity and stability of the SERS-active membrane

SERS is an important analytical method that can be used to obtain fingerprint information by studying vibrational and rotational modes of a system. The uniformity, stability and reproducibility of the active substrate are crucial for SERS

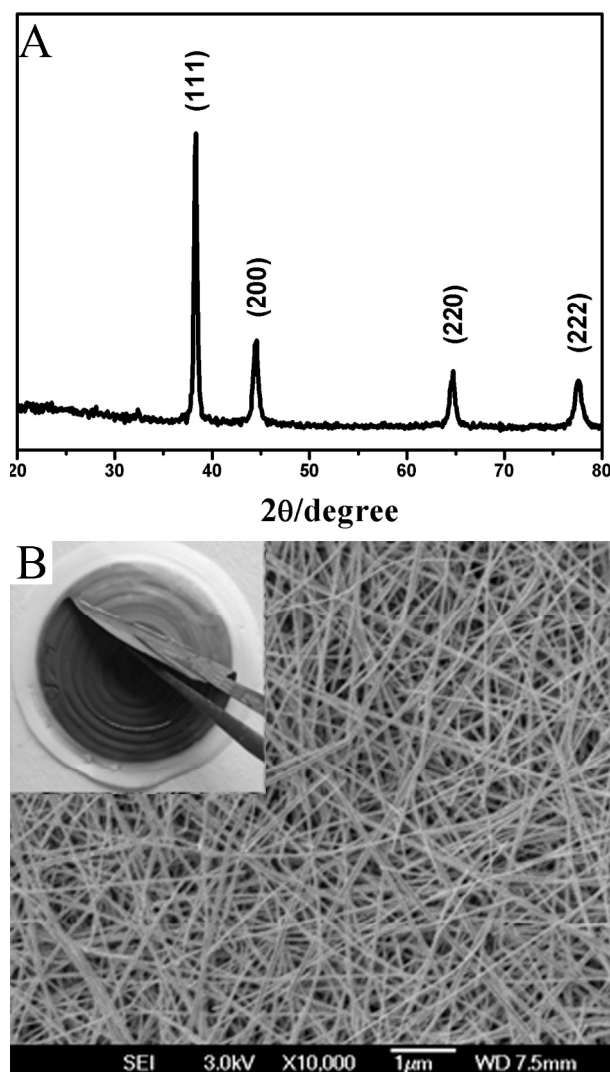


Fig.2 (A) XRD pattern of silver nanowires compared to a standard JCPDS card no. 04-0783 for Ag. (B) SEM image of silver nanowires loaded on the filter membrane. Inset shows the photo of the extraction membrane.

detection.<sup>40-42</sup> To illustrate the uniformity of the active substrate, the SERS intensity of PATP with the concentration of  $10 \mu\text{g}\cdot\text{mL}^{-1}$  were recorded under laser radiation with laser powers at 180 mw, as shown in Fig.3A. The uniformity of this membrane for SERS detection was evaluated by randomly selecting twenty-four points on a single substrate and recording their corresponding SERS spectra. The inset image of Fig.3A shows the intensity change of the Raman bands at  $1076 \text{ cm}^{-1}$ , and the relative standard deviation of the intensity is 4.1% from twenty-four different points, which indicated the uniformity of the substrate was fairly good.

The temporal stability of the substrate under continuous laser radiation is also essential parameter for SERS detection. To illustrate the temporal stability of the active substrate, the SERS spectra of PATP with the concentration of  $10 \mu\text{g}\cdot\text{mL}^{-1}$  were recorded under continuous laser radiation for 130 seconds, as shown in Fig.3B. The spectra were recorded every 5 s and the integration time was 1 s. It was shown that the overall shape had no obvious change, and the bands intensity of the SERS had

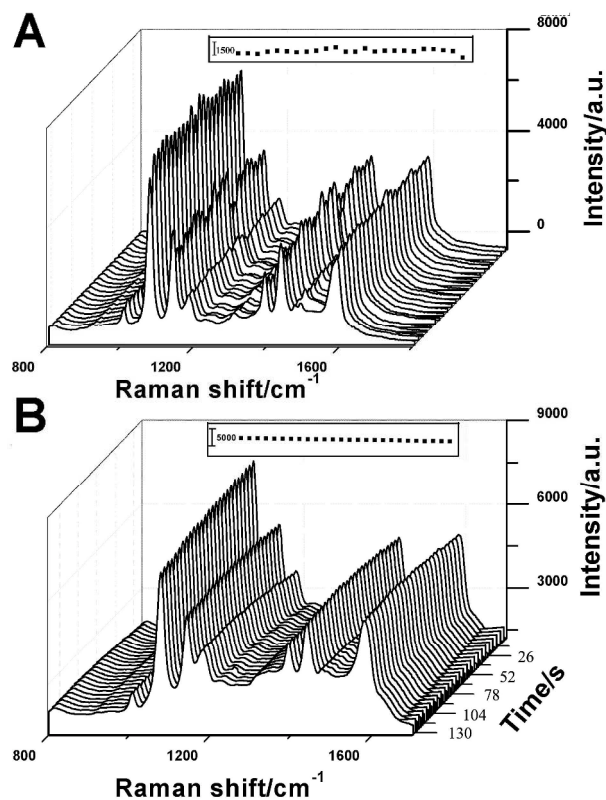


Fig.3 (A) The uniformity and (B) laser irradiation stability of the substrate probed with  $10 \mu\text{g}\cdot\text{mL}^{-1}$  PATP. Inset shows the intensity change of the Raman band centered at  $1076 \text{ cm}^{-1}$ .

small change during the laser irradiation. The inset image of Fig.3B shows the intensity change of the Raman bands at  $1076 \text{ cm}^{-1}$ , the relative standard deviation of 6.2%. These results indicated that the substrate had a good temporal stability under continuous laser radiation, which could meet the requirements of routine SERS detection.

### SPE-SERS detection

Solid-phase extraction (SPE), which is a simple and rapid pre-concentrate process, is commonly used to pre-concentrate organic chemicals and heavy metal ions in water or in food analysis.<sup>3</sup> Here, silver nanowires membrane had good Raman performance due to present of Raman “hot spot”, so it could combine the advantages of SPE and SERS technology.

In Fig.4, the SERS detection performance of the membrane by filtering is compared with that by the immersion method. The measured Raman signals in Fig.4 show that the signal intensity by filtering 5 mL PATP ( $10 \mu\text{g}\cdot\text{mL}^{-1}$ ) is better than that by immersing the same sample. Thus, for the case of PATP, the SERS-active extraction membrane enables a good improvement in detection performance compared to immersing SERS measurements.

Fig.5 presents the detection performance of the silver nanowires membrane for PATP. To obtain the lowest detection concentration for PATP using the SPE-SERS technique, we prepared different concentration dilutions of PATP in water. Fig.5A shows that the lowest detected concentrations of PATP is

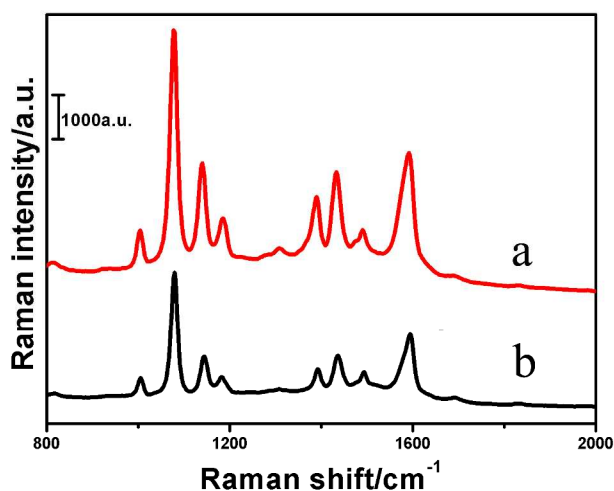


Fig.4 Comparison of measured SERS spectra for PATP by (a) filtering and (b) immersing PATP in aqueous solution.

0.001  $\mu\text{g}\cdot\text{mL}^{-1}$ , which should be owing to the fact that the PATP molecules were adsorbed on the substrate. The quantitative SERS analysis was showed in Fig.5B and S8. Data points representing

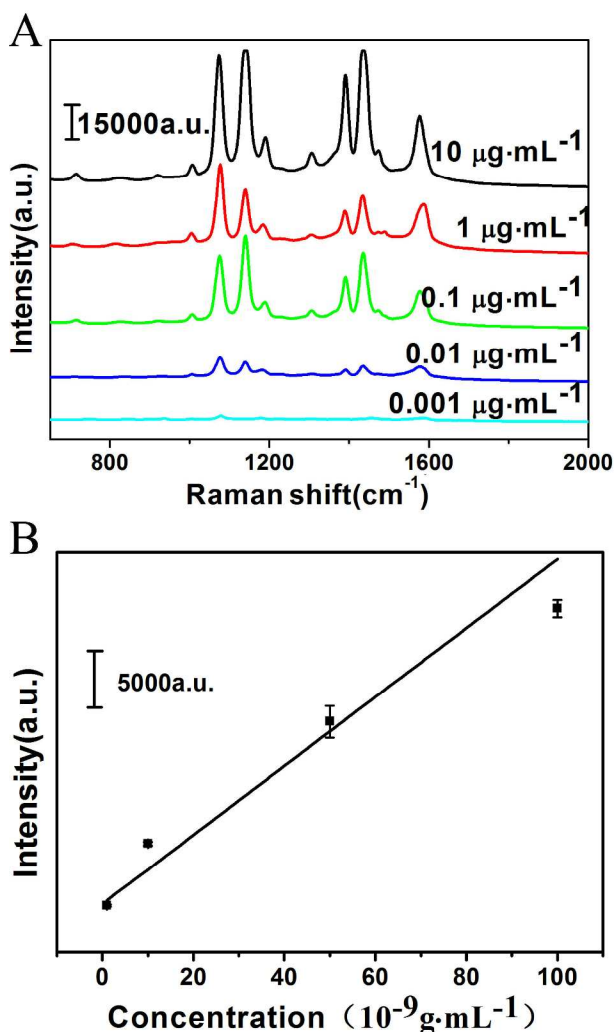


Fig.5 (A) SERS spectra of the different concentrations PATP in aqueous solution adsorbed on the membrane by flow-through method. (B) The SERS intensity of the 1076  $\text{cm}^{-1}$  peak for different PATP concentrations.

the peak height of the 1076  $\text{cm}^{-1}$  PATP Raman peak increased consistently with the increasing of aqueous PATP concentrations in Fig.S9. In the plot, the data points represent the mean value for two separate membranes for obtaining relative accurate results. It could be seen that the plot of the intensity of the 1076  $\text{cm}^{-1}$  band versus the concentration of PATP shows a monotonic increase of the intensity at the lower concentration, the peak intensity remained unchanged at the higher concentration, which arose from the saturation of the active sites of the enhancing substrate. It is noted that the Raman peak intensity at 1076  $\text{cm}^{-1}$  versus a series of PATP concentrations yielded a good linear relationship in the concentration range of 0.1 to 0.001  $\mu\text{g}\cdot\text{mL}^{-1}$ , as shown in Fig.5B.

Phorate is an organophosphate pesticide effectively against a wide array of insects, mites, and some nematodes. It has been also classified by the U.S. Environmental Protection Agency as a restricted use pesticide because of its high toxicity to reptiles, birds, and fish.<sup>43</sup> Thus, it is critical to monitor the concentration of phorate to ensure the best treatment. The spectrum of phorate shows feature Raman bands at 527, 635, 761, 1097, 1284 and 1392  $\text{cm}^{-1}$  in Fig. S7A. The bands of intensity appearing at 635 and 1284  $\text{cm}^{-1}$  may be assigned to  $\nu(\text{C}-\text{S})$ . The peaks at 761, 1097 and 1392  $\text{cm}^{-1}$  are assigned as  $\nu(\text{P}-\text{O})$ ,  $\nu(\text{C}-\text{C})$  and  $\nu(\text{P}-\text{O}-\text{C})$ .<sup>44</sup>

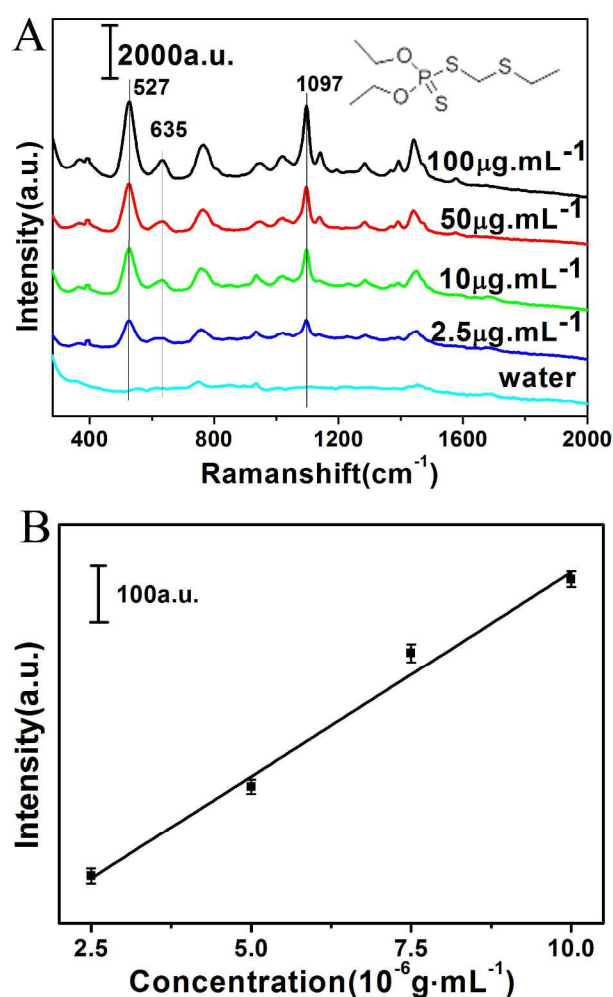


Fig.6 (A) SERS spectra of the different concentrations phorate in aqueous solution with obtained by filtered method. (B) The intensity of the 1097  $\text{cm}^{-1}$  SERS peak for different phorate concentrations.

SERS spectra of phorate molecules at different concentrations are shown in Fig.6A. It is revealed that phorate can be detected even at  $2.5 \mu\text{g}\cdot\text{mL}^{-1}$ , which should be owing to the fact that phorate molecules were adsorbed onto the substrate. Fig.S9 showed the calibration curve and simulation curve for phorate of the SERS intensity at  $1097 \text{ cm}^{-1}$ . The results reveal that the intensity of the band decreased with diluted samples, which indicates that the enrichment capacity of the extraction membrane was unsaturated at lower concentrations. The Raman intensity reached a platform when the concentration of phorate is more than  $1.0 \times 10^{-4} \text{ g}\cdot\text{mL}^{-1}$  in Fig. S9B, which results from the saturation of the enrichment capacity of the substrate. Fig.6B shows the Raman intensity of phorate at  $1097 \text{ cm}^{-1}$  versus its concentration in the range from 10 to  $2.5 \mu\text{g}\cdot\text{mL}^{-1}$ , which reveals a good linear correlation.

Melamine is a nitrogen-rich compound mainly used to produce kitchenware, commercial filters, flame retardants, and other products. Its wide use may result in the presence of trace amounts of melamine in the food supply.<sup>45, 46</sup> Melamine was detected to further demonstrate that the flow-through method on extraction membrane is quantitative. Compared to the background Raman

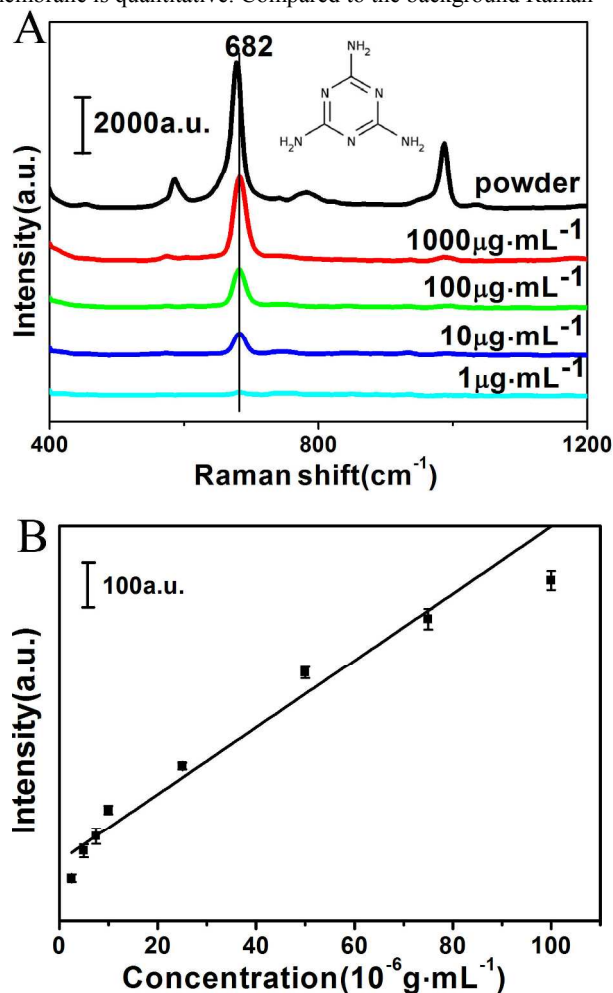


Fig.7 (A) SERS spectra of the different concentrations melamine in aqueous solution absorbed on the membrane by flow-through method. (B) The intensity of the  $682 \text{ cm}^{-1}$  SERS peak for different melamine concentrations.

band, the Raman peak of melamine at  $682 \text{ cm}^{-1}$  is assigned to the ring breathing mode in the Fig.S7B.<sup>45</sup> Fig.7A showed the Raman spectra of melamine, the lowest measured concentration was  $1 \mu\text{g}\cdot\text{mL}^{-1}$  for the extraction membrane. Fig.S10 showed the calibration curve and simulation curve for melamine of the SERS intensity at  $682 \text{ cm}^{-1}$ . The Raman intensity reached a platform when the concentration of melamine is more than  $1.0 \times 10^{-3} \text{ g}\cdot\text{mL}^{-1}$  in Fig. S10B, which results from the saturation of the enrichment capacity of the substrate. Fig.7B showed the Raman intensity of melamine at  $1097 \text{ cm}^{-1}$  versus its concentration in the range from 1 to  $100 \mu\text{g}\cdot\text{mL}^{-1}$ , which reveals a good linear correlation.

The experimental results were theoretically analysed. The optical extinction cross section of the two silver nanowires was simulated by finite-different time-domain (FDTD) as shown in Fig.S11. For the FDTD calculation, the diameter of the model of silver nanowires is set to the average experimental results of 50 nm. The electromagnetic radiation used was a total field scattered field source, provided by the software, which is useful for solving scattering problems. The source separates the simulation area into two parts: (1) the y-z mode; (2) the x-y mode. It can be seen from the Fig.S11 that the intersection of the silver nanowires has more highly electric-field intensity enhancement. This simple model has practical advantages for locating and visualizing electric-field “hot spots” for SERS applications.

## Conclusions

We have fabricated a highly sensitive SERS-active silver nanowires membrane via filtering silver nanowires colloid, which was used for SERS detection of contaminants. This membrane had good Raman performance due to present of Raman “hot spot”. The membrane also showed rapid extraction speed for the contaminants. In addition, quantitative analysis of the samples in aqueous solution was performed using this membrane. The Raman intensity versus the samples concentration yielded a good linear relationship. The linear relationship of PATP, phorate and melamine existed in the concentration range of 0.001 to  $0.1 \mu\text{g}\cdot\text{mL}^{-1}$ ,  $2.5$  to  $10 \mu\text{g}\cdot\text{mL}^{-1}$  and  $1$  to  $100 \mu\text{g}\cdot\text{mL}^{-1}$  respectively. These above results indicated that the SERS-active extraction membrane had good stability, uniformity and high SERS activity, suggesting that the extraction membrane was a promising candidate for rapid detection of food organic contaminants.

## Acknowledgments

We thank the financial support from National Basic Research Program of China (973 Program 2013CB934301), National Natural Science Fund of China (NSFC 50972083 21377068 and 91023011), Shandong Provincial Natural Science Foundation for Distinguished Young Scholars (JQ201004) and Independent Innovation Foundation of Shandong University (IIFSDU-2012JC027).

## Notes and references

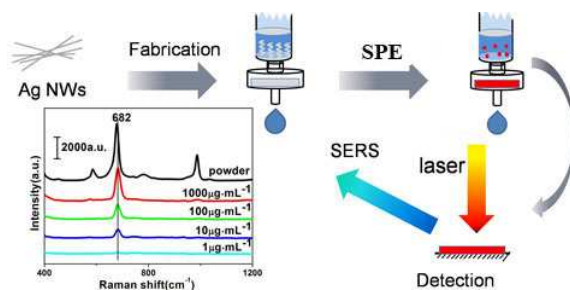
a Key Laboratory for Colloid & Interface Chemistry of Education Ministry, Department of Chemistry, Shandong University, Jinan Shandong, 250100, P. R. China. E-mail: [jhzhan@sdu.edu.cn](mailto:jhzhan@sdu.edu.cn)

*b Department of Physics, Xiamen University, Xiamen Fujian, 361005, P. R. China.*

† Electronic Supplementary Information (ESI) available: [details of any supplementary information available should be included here]. See DOI: 10.1039/b000000x/.

1. T.V. Duncan, *J. Colloid Interface Sci.*, 2011, **363**, 1–24.
2. R. Mcgorrin, *J. Agric. Food Chem.*, 2009, **57**, 8076–8088.
3. W. Andersen, S. Turnipseed, J. Roybal, *J. Agric. Food Chem.*, 2006, **54**, 4517–4523.
4. Z. Xiong, L. Zhang, R. Zhang, Y. Zhang, J. Chen and W. Zhang, *J. Sep. Sci.*, 2012, **35**, 2430–2437.
5. Y. Cai, G. Jiang, J. Liu and Q. Zhou, *Anal. Chim. Acta*, 2003, **494**, 149–156.
6. M. E. Lindsey, M. Meyer and E. Thurman, *Anal. Chem.*, 2001, **73**, 4640–4646.
7. M. Flores, R. Romero-González, A. Frenich and J. Vidal, *Food Chem.*, 2012, **134**, 2465–2472.
8. H. Niu, Y. Cai, Y. Shi, F. Wei, J. Liu, S. Moua and G. Jiang, *Anal. Chim. Acta*, 2007, **594**, 81–92.
9. Y. Cai, G. Jiang, J. Liu, Q. Zhou, *Anal. Chem.*, 2003, **75**, 2517–2521.
10. J. Kneipp, H. Kneipp, K. Kneipp, *Chem. Soc. Rev.*, 2008, **37**, 1052–1060.
11. Y. Li, L. Qu, D. Li, Q. Song, F. Fathi, Y. Long, *Biosens. Bioelectron.*, 2013, **43**, 94–100.
12. L. Qian, R. Mookherjee, *Nano Res*, 2011, **4**(11), 1117–1128.
13. C. Zhu, G. Meng, Q. Huang, Z. Huang, *J. Hazard. Mater.*, 2012, **211–212**, 389–395.
14. B. Liu, G. Han, Z. Zhang, R. Liu, C. Jiang, S. Wang and M. Han, *Anal. Chem.*, 2012, **84**, 255–261.
15. V. Joseph, C. Engelbrekt, J. Zhang, U. Gernert, J. Ulstrup, J. Kneipp, *Angew. Chem. Int. Ed.*, 2012, **51**, 7592–7596.
16. D. Jeong, Y. Zhang and M. Moskovits, *J. Phys. Chem. B*, 2004, **108**, 12724–12728.
17. J. Yuan, Y. Lai, J. Duan, Q. Zhao and J. Zhan, *J. Colloid Interface Sci.*, 2012, **365**, 122–126.
18. K. Kneipp, M. Moskovits and H. Kneipp, *Eds. Springer: Heidelberg and Berlin*, 2006.
19. J. Li, Y. Huang, Y. Ding, Z. Yang, S. Li, X. Zhou, F. Fan, W. Zhang, Z. Zhou, D. Wu, B. Ren, Z. Wang and Z. Tian, *Nature*, 2010, **464**, 392–395.
20. X. Han, B. Zhao and Y. Ozaki, *Anal. Bioanal. Chem.*, 2009, **394**, 1719–1727.
21. M. Knauer, N. Ivleva, X. Liu, R. Niessner and C. Haisch, *Anal. Chem.*, 2010, **82**, 2766–2772.
22. R. Halvorson and P. Vikesland, *Environ. Sci. Technol.*, 2010, **44**, 7749–7755.
23. X. Jiang, Y. Lai, M. Yang, H. Yang, W. Jiang and J. Zhan, *Analyst*, 2012, **137**, 3995–4000.
24. S. Lee, A. Morrill and M. Moskovits, *J. Am. Chem. Soc.*, 2006, **128**, 2200–2201.
25. H. J. Chen, X. S. Kou, Z. Yang, W. H. Ni, J. F. Wang, *Langmuir*, 2008, **24**, 5233–5237.
26. C. Lee, M. Hankus, L. Tian, P. Pellegrino and S. Singamaneni, *Anal. Chem.*, 2011, **83**, 8953–8958.
27. W. Wei and I. White, *Analyst*, 2012, **137**, 1168–1173.
28. Y. Meng, Y. Lai, X. Jiang, Q. Zhao and J. Zhan, *Analyst*, 2013, **138**, 2090–2095.
29. L. Cui, M. Yao, B. Ren and K. Zhang, *Anal. Chem.*, 2011, **83**, 1709–1716.
30. W. Wei and I. White, *Anal. Chem.*, 2010, **82**, 9626–9630.
31. K. Zhang, H. Zhou, Q. Mei, S. Wang, G. Guan, R. Liu, J. Zhang and Z. Zhang, *J. Am. Chem. Soc.*, 2011, **133**, 8424–8427.
32. Q. Mei and Z. Zhang, *Angew. Chem. Int. Ed.*, 2012, **51**, 5602–5606.
33. A. Tao, F. Kim, C. Hess, J. Goldberger, R. He, Y. Sun, Y. Xia and P. Yang, *Nano Lett.*, 2003, **3**, 1229–1233.
34. S. De, T. Higgins, P. Lyons, E. Doherty, P. Nirmalraj, W. Blau, J. Boland and J. Coleman, *ACS nano*, 2009, **3**, 1767–1774.
35. R. Aroca, P. Goulet, D. Santos, R. Alvarez-Puebla and O. Oliveira, *Anal. Chem.*, 2005, **77**, 378–382.
36. E. Formo, S. Mahurin and S. Dai, *ACS Appl. Mater. Interfaces*, 2010, **2**, 1987–1991.
37. A. Madaria, A. Kumar, F. Ishikawa and C. Zhou, *Nano Res.*, 2010, **3**, 564–573.
38. Q. Luu, J. Doorn, M. Berry, C. Jiang, C. Lin and P. May, *J. Colloid Interface Sci.*, 2011, **356**, 151–158.
39. P. S. Mdluli, N. Revaprasadu, *J. Alloy. Compd.*, 2009, **469**, 519–522.
40. R. Que, M. Shao, S. Zhuo, C. Wen, S. Wang and S. Lee, *Adv. Funct. Mater.*, 2011, **21**, 3337–3343.
41. L. Qu, D. Li, J. Xue, W. Zhai, J. Fossey and Y. Long, *Lab Chip*, 2012, **12**, 876–881.
42. L. Qu, Y. Li, D. Li, J. Xue, J. Fossey and Y. Long, *Analyst*, 2013, **138**, 1523–1528.
43. R. Lavado, L. Maryoung and D. Schlenk, *Environ. Sci. Technol.*, 2011, **45**, 4623–4629.
44. H. J. Kim, C. J. Lee, M. R. Karim, M. S. Kim, M. S. Lee, *Spec. chim. Acta Part A*, 2011, **78**, 179–184.
45. A. Kim, S. Barcelo, R. Williams and Z. Li, *Anal. Chem.*, 2012, **84**, 9303–9309.
46. World Health Organization, Melamine and Cyanuric Acid: Toxicity, Preliminary Risk Assessment and Guidance on Levels in Food, October 3, 2008.

TOC Figure



1  
2  
3  
4  
5  
6  
7  
8  
9  
10  
11  
12  
13  
14  
15  
16  
17  
18  
19  
20  
21  
22  
23  
24  
25  
26  
27  
28  
29  
30  
31  
32  
33  
34  
35  
36  
37  
38  
39  
40  
41  
42  
43  
44  
45  
46  
47  
48  
49  
50  
51  
52  
53  
54  
55  
56  
57  
58  
59  
60